www.czasopisma.pan.pl PAN POLSKA AKADEMIA NAUK www.journals.pan.pl

A R C H I V E S O F M E T A L L U R G Y A N D M A T E R I A L S

Volume 56 2011 Issue 4

DOI: 10.2478/v10172-011-0121-x

K. OSIŃSKA*, M. ADAMCZYK*, J. DZIK*, H. BERNARD*, D. CZEKAJ*

FABRICATION AND CHARACTERIZATION OF BST60/40//PVDF CERAMIC-POLYMER COMPOSITE

OTRZYMYWANIE I CHARAKTERYSTYKA KOMPOZYTÓW CERAMICZNO-POLIMEROWYCH BST60/40//PVDF

In this paper BST//PVDF composites with 0-3 connectivity were prepared from $(Ba_{0.6}Sr_{0.4})O_3$ (BST60/40) ceramic powder and polyvinylidene fluoride (PVDF) powder by a hot pressing method, for different concentration of the ceramic phase (c_V). Morphology of BST//PVDF composites was observed by transmission electron microscopy and scanning electron microscopy, whereas the crystalline structure was studied by the X-ray diffraction method. The temperature dependence of dielectric permittivity of BST//PVDF composites was measured in the frequency range of f=10kHz-1MHz. The split-post dielectric resonator (SPDR) was used for the measurements of the real and imaginary part of dielectric permittivity of BST//PVDF composites in the microwave frequency range of f=3-10GHz. It was found, that the dielectric properties of the ceramic-polymer composite for c_V >20% change significantly for both small (f=10kHz-1MHz) and high (f=3-10GHz) frequencies. The abrupt increase in permittivity may indicate an excess of the percolation threshold, so the ceramic-polymer composite for the concentrations of the active ceramic phase c_V >20% cannot be indexed as composites with 0-3 connectivity.

Keywords: BST, PVDF, ceramic-polymer composite, dielectric permittivity

W ramach prezentowanej pracy, kompozyty BST//PVDF, o sposobie łączenia faz 0-3, otrzymywane były z proszku ceramicznego $(Ba_{0.6}Sr_{0.4})O_3$ (BST60/40) oraz proszku poli(fluorku winylidenu) (PVDF), dla różnego stężenia fazy ceramicznej (c_V), metodą prasowania na gorąco. Morfologię kompozytów BST//PVDF obserwowano z zastosowaniem transmisyjnego oraz skaningowego mikroskopu elektronowego. Strukturę krystaliczną badano metodą dyfrakcji promieniowania rentgenowskiego. Temperaturowa zależność przenikalności elektrycznej mierzona była w zakresie częstotliwości f=10kHz-1MHz. Do pomiarów w zakresie bardzo wysokich częstotliwości f=3-10GHz zastosowano rezonator dielektryczny SPDR. Można zauważyć, że zarówno dla niskich (f=10kHz-1MHz), jak i wysokich (f=3-10GHz) częstotliwości właściwości dielektryczne kompozytów ceramiczno-polimerowych dla stężenia fazy ceramicznej c_V >20%, zmieniają się w znacznym stopniu. Gwałtowny wzrost wartości przenikalności może świadczyć o przekroczeniu progu perkolacji, a więc kompozyty ceramiczno-polimerowe o stężeniu aktywnej fazy ceramicznej c_V >20% nie mogą być indeksowane jako kompozyty o sposobie łączenia faz 0-3.

1. Introduction

Composites are many–phase systems, the properties of which are determined by the number of phases, the volumetric fraction the properties of individual phases and by the way in which the different phases are interconnected. A particular property of the composite may depend on several properties of the individual phases (combinational property) [1].

Two–phase composites consist of an active phase (reinforcement) and non-active (passive) phase (matrix). Functional composites which are used in electronics utilize mainly BT, PT, PZT and other solid solutions with admixtures as the active ceramic phase, whereas the passive phase is constituted from polymer like PVC, PVDF, PE, PP, PS, P(OV-CV), P(VDF–TrFE) [2].

Composites that are constituted from electroceramics and polymer have gained a widespread application in a number of electromechanical transducers such as hydrophones, vibration sensors, pressure and stress sensors, actuators, transducer for medical ultrasonic imaging, transistors MOS, capacitor, Peltiera's element [3].

Newnham et al. established the notation for describing the number of dimensions that each phase is physically in contact with itself. To date, ten different types of two–phase electro composites have been studied: 0-0, 0-1, 0-2, 0-3, 1-1, 1-2, 1-3, 2-2, 2-3, 3-3 [2, 4].

* UNIVERSITY OF SILESIA, DEPARTMENT OF MATERIALS SCIENCE, 41-200 SOSNOWIEC, 2 ŚNIEŻNA STR., POLAND

The simplest type of the composites is that with 0-3 connectivity. Such a composite consists of the there–dimensionally connected polymer matrix loaded with piezoelectrically active ceramic particles. In 0-3 connectivity the ceramic particles are not in contact with each other and the polymer phase is self–connected in all directions [5, 6].

In the present study attention is confined to one of the most commonly encountered connectivity 0-3. The ceramic-polymer composite exhibiting the 0-3 connectivity, with different concentration of ceramic phase, has been fabricated on the base of sol-gel derived barium strontium titanate electroceramic powder $Ba_{0.6}Sr_{0.4}TiO_3$ (BST60/40) and polyvinylidene fluoride (PVDF) polymer, by the hot pressing method. Results of influence of the ferroelectric ceramic phase on microstructure, crystalline structure and dielectric properties of ceramic-polymer composite with volume fraction of the active phase from c_V=1.47% up to c_V=60% are also reported.

2. Experimental

In the present work the BST60/40//PVDF ceramic-polymer composites of volumetric content c_V=1.47%, 3.04%, 4.75%, 6.60%, 10%, 20%, 50% and 60% and 0-3 connectivity were prepared in the form of disks. $Ba_{0.6}Sr_{0.4}TiO_3$ powder was obtained by the sol-gel method from barium acetate ($Ba(CH_3COO)_2$, SIGMA-ALDRICH 99%), strontium acetate ($Sr(CH_3COO)_2$, SIGMA-ALDRICH 99%), and tetra-butyl titanate ($Ti(OC_4H_9)_4$, SIGMA-ALDRICH 97%) as starting materials according to the method described elsewhere [7, 8]. Glacial acetic acid (CH_3COOH, POCH 99.9%) and n-butyl alcohol (C_4H_9OH, POCH 99.9%) were used as solvents. The temperature of calcinations of the amorphous BST gel was T=850°C (soaking time t=4h), whereas the temperature of sintering was T=1450°C (soaking time t=4h).

The BST60/40//PVDF ceramic-polymer composite samples was fabricated by the hot pressing method from BST60/40 ceramic powder and PVDF powder at T=145°C, p=120MPa [5, 6].

The morphology of BST//PVDF composites was observed by transmission electron microscopy Philips EM 400T and scanning electron microscopy HITACHI S-4700. The crystal structure was examined by X-ray diffraction with CoK_α radiation (Θ-2Θ method, scan step size $\Delta\Theta$=0.02 deg, scan type continuous, scan step time t=4s) at room temperature.

For electric measurements, composite samples of h=1mm thick and d=20mm in diameter were covered with silver paste electrodes. The dielectric properties of PVDF polymer and ceramic- polymer composites were studied with the impedance gain/phase analyser HP4192A in the frequency range from f=10kHz to f=1MHz. The measurements were performed with heating from T=-50°C to T=200°C at a rate of ν=1deg/min.

3. Results and discussion

Transmission (a) and scanning (b) electron micrographs of PVDF polymer, 1.47%BST60/40//PVDF, 6.60%BST60/40//PVDF, 20%BST60/40//PVDF and 50%BST60/40//PVDF composites are given in Fig. 1, Fig. 2, Fig. 3, Fig. 4, Fig. 5, respectively. One can see that polymer grains are arranged around the ceramic grains. The BST60/40 powder is well dispersed in the PVDF polymer matrix without serious powder agglomeration.

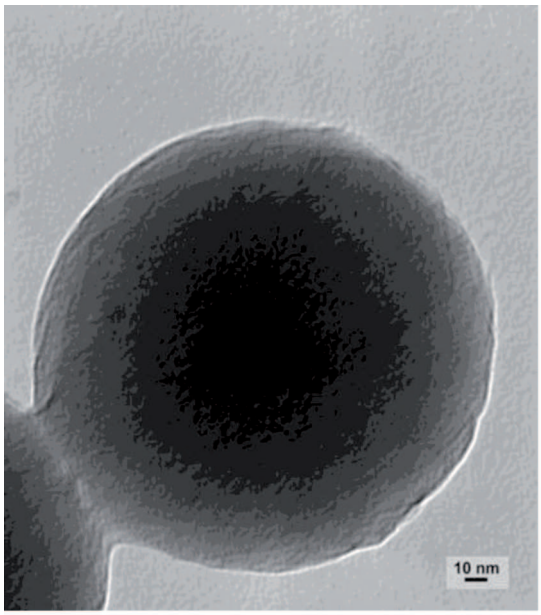

Fig. 1a. TEM micrograph of PVDF polymer

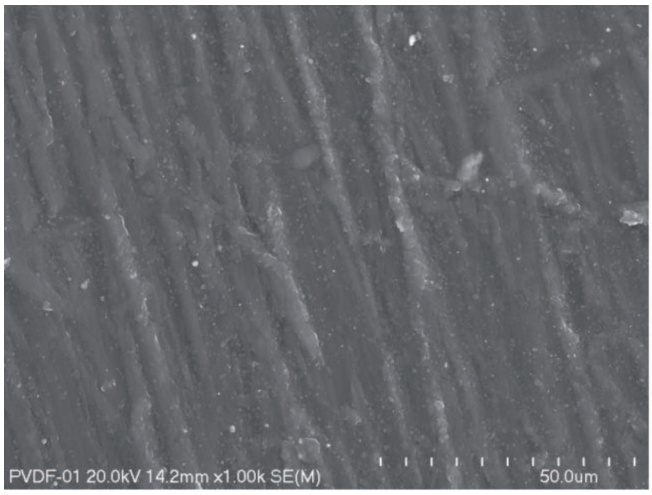

Fig. 1b. SEM micrograph of PVDF polymer

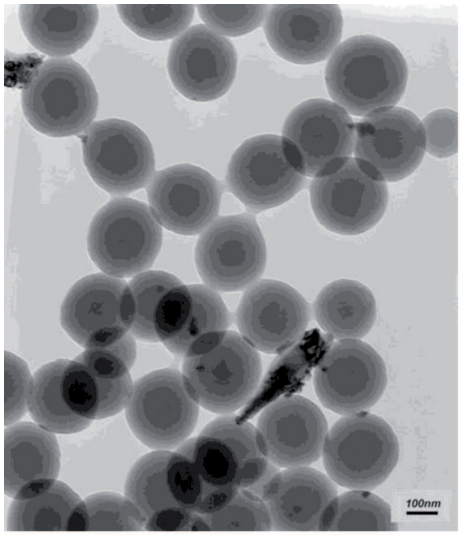

Fig. 2a. TEM micrograph of 1.47%BST60/40//PVDF composite

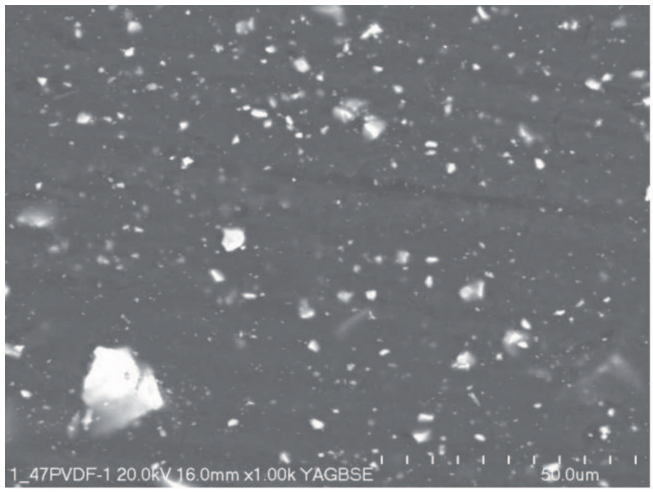

Fig. 2b. SEM micrograph of 1.47%BST60/40//PVDF composite

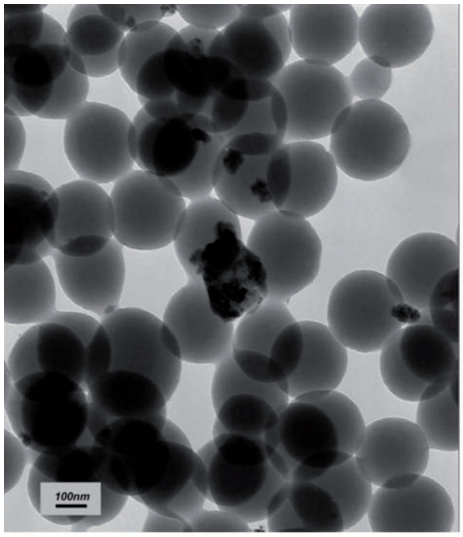

Fig. 3a. TEM micrograph of 6.6%BST60/40//PVDF composite

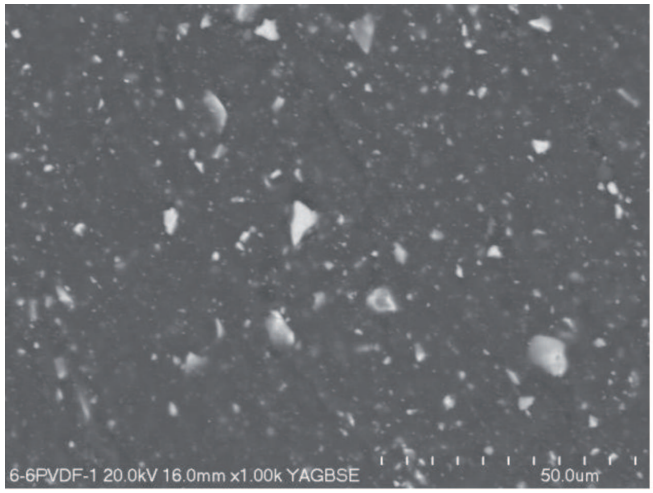

Fig. 3b. SEM micrograph of 6.6%BST60/40//PVDF composite

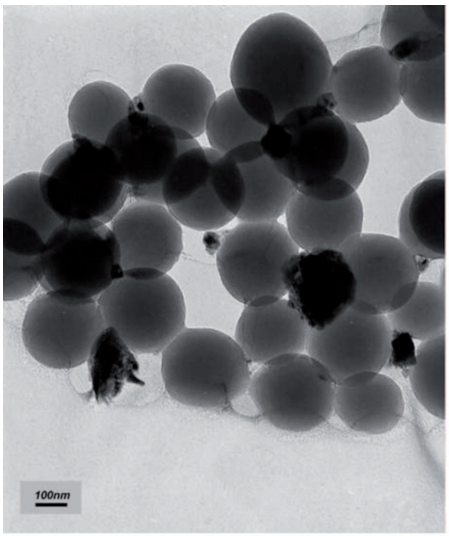

Fig. 4a. TEM micrograph of 20%BST60/40//PVDF composite

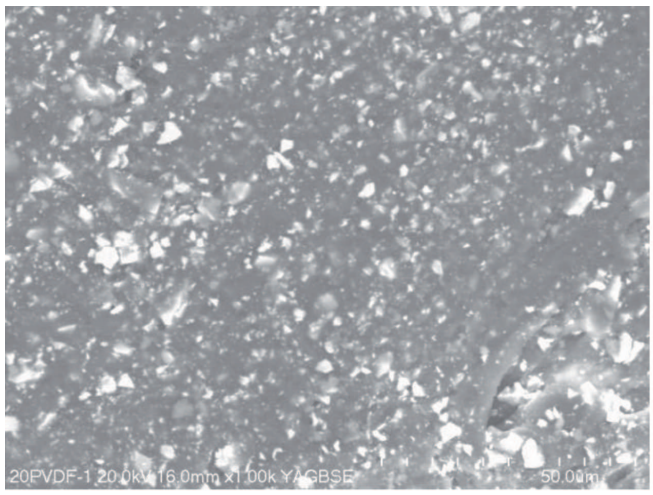

Fig. 4b. SEM micrograph of 20%BST60/40//PVDF composite

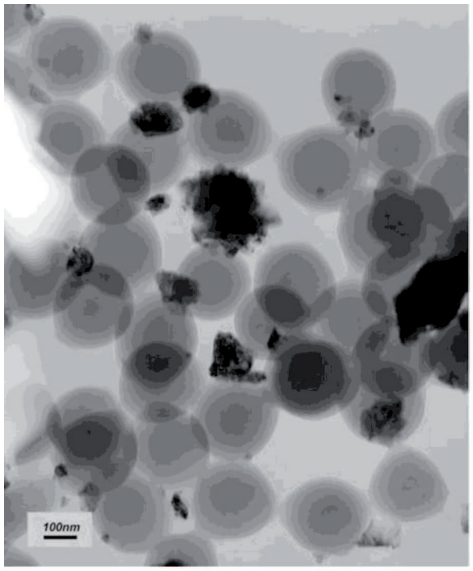

Fig. 5a. TEM micrograph of 50%BST60/40//PVDF composite

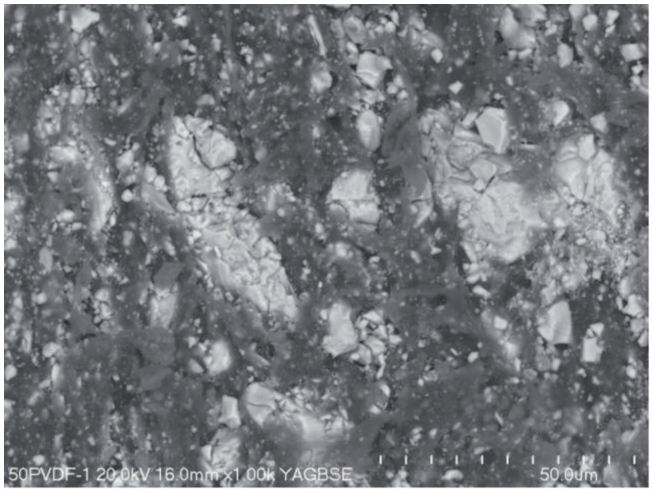

Fig. 5b. SEM micrograph of 50%BST60/40//PVDF composite

X-ray diffraction spectra of PVDF polymer and BST60/40//PVDF composite are in Fig. 6. X-ray phase analysis for 6.60%BST60/40//PVDF composite is shown in Fig. 7 and X-ray diffraction spectrum for 6.60%BST60/40//PVDF composite with lines for barium strontium titanate and polyvinylidene fluoride are shown in Fig. 8.

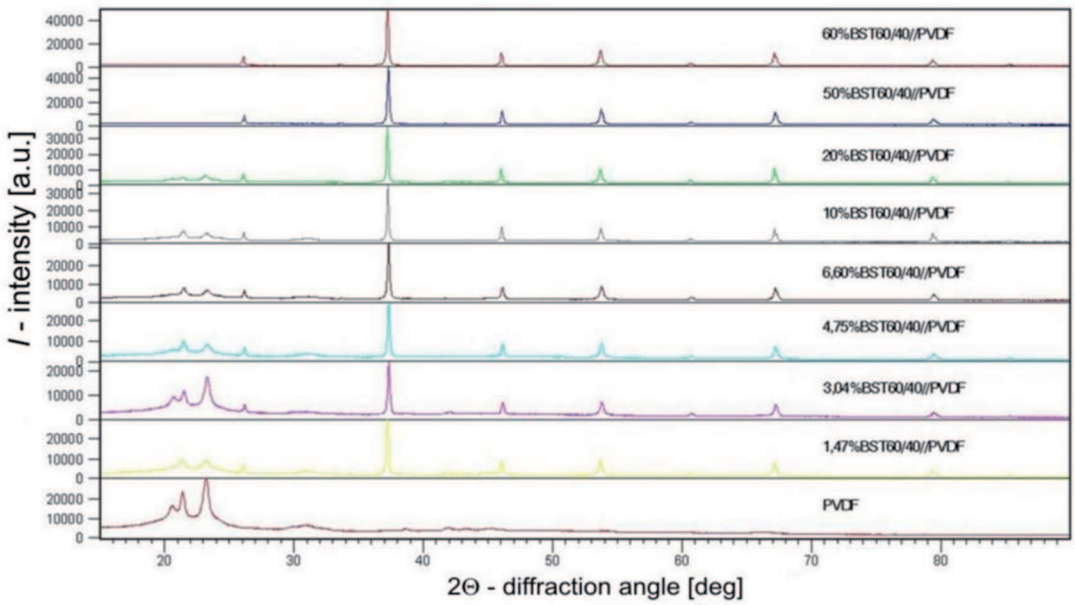

Fig. 6. X-ray diffraction patterns of PVDF polymer and BST60/40//PVDF composite

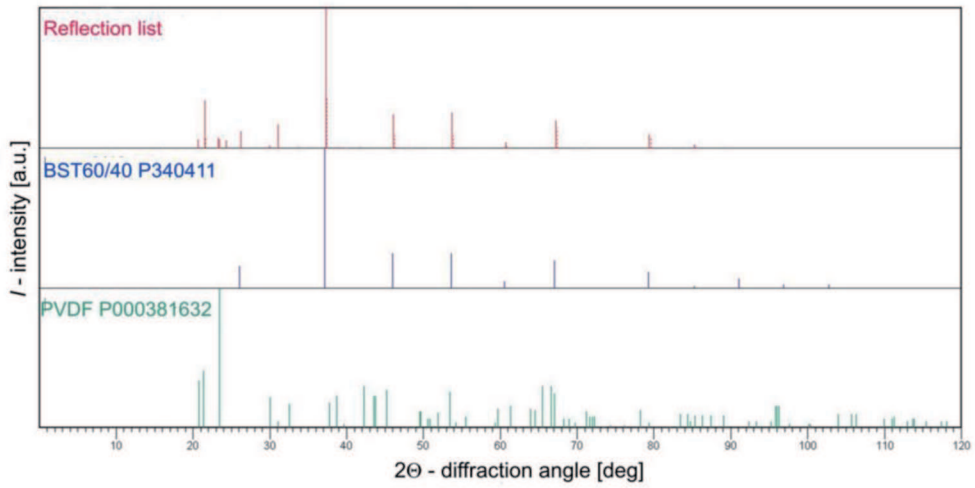

Fig. 7. X-ray phase analysis for 6.60%BST60/40//PVDF composite

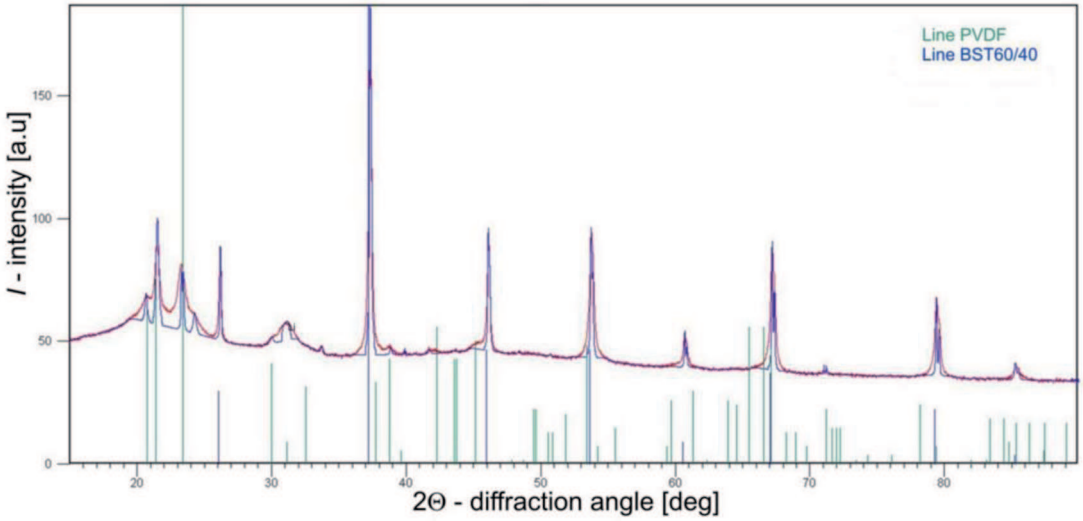

Fig. 8. X-ray diffraction pattern for 6.60%BST60/40//PVDF composite with diffraction lines for barium strontium titanate and polyvinylidene fluoride taken from data base

Identification of the phases constituting the composite have shown agreement in positions of the diffraction lines of the ceramic phase ($Ba_{0.6}Sr_{0.4}TiO_3$-PDF card No 340411) and polymer phase ($(C_2H_2F_2)_n$-PDF card No 000381632) with the experimental spectrum of the BST60/40//PVDF ceramic-polymer composite.

The knowledge of the dielectric response of the ceramic-polymer composites is essential because the permittivity is involved in the "figure of merit" (FOM) of the physical quantities important for particular applications. In the case of supposed piezoelectric applications, the FOM is described by the formula (1) and (2) [1, 3]:

$$FOM = d_h \times g_h, \tag{1}$$

$$g_h = \frac{d_h}{\varepsilon_0 \times \varepsilon'} \tag{2}$$

g_h – hydrostatic piezoelectric voltage coefficient,
d_h – hydrostatic piezoelectric coefficient,
ε_0 – permittivity of vacuum,
ε' – permittivity of material.

Therefore, the possible use of ceramic-polymer composite for piezoelectric applications depends strongly on dielectric response.

Dependence of the real ε' (a) and imaginary ε'' (b) part of dielectric permittivity on temperature for BST60/40 electroceramic powder used for composite fabrication is given in Fig. 9. It can be seen from Fig. 9 that the three peaks originated from cubic-tetragonal, tetragonal-orthorhombic and orthorhombic-rhombohedral phase transition.

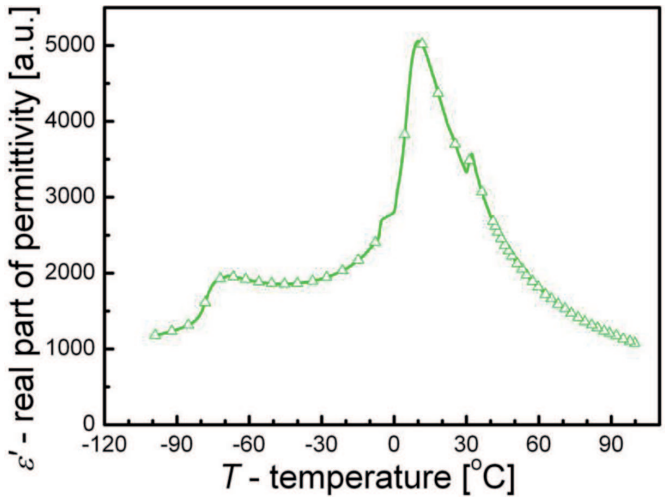

Fig. 9a. Temperature dependence of the real part of dielectric permittivity ε' for BST60/40 ceramic at f=100kHz

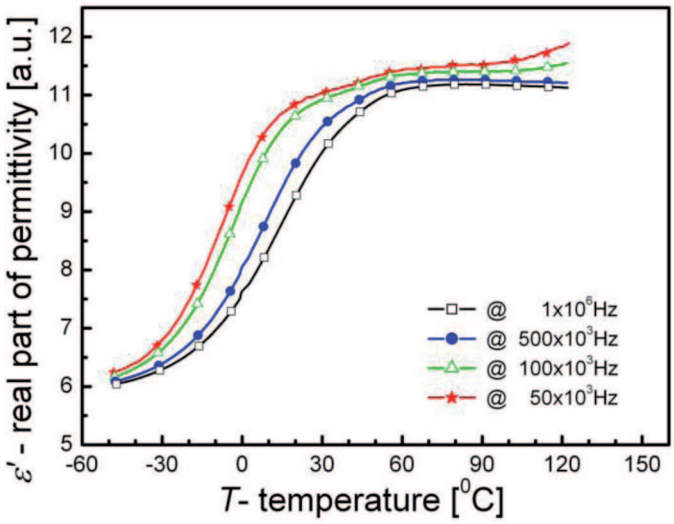

Fig. 10a. Temperature dependence of the real part of dielectric permittivity ε' for polyvinylidene fluoride PVDF

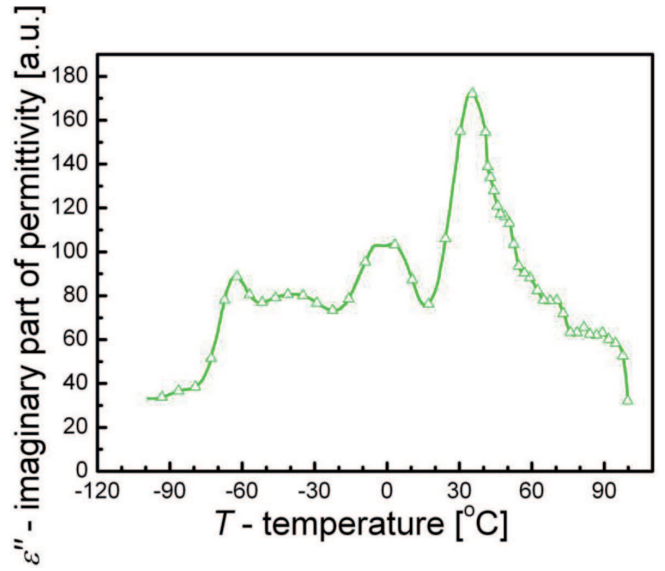

Fig. 9b. Temperature dependence of imaginary part of dielectric permittivity ε" for BST60/40 ceramic at f=100kHz

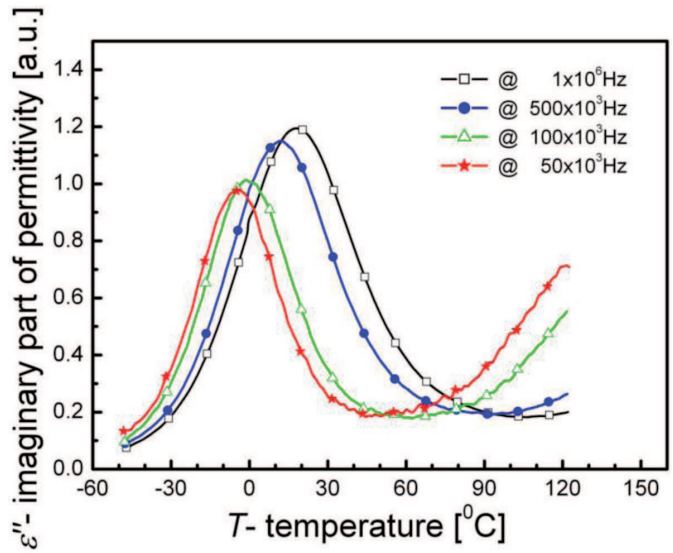

Fig. 10b. Temperature dependence of the imaginary part of dielectric permittivity ε" for polyvinylidene fluoride PVDF

Dielectric dispersion (ε') and absorption (ε") of polyvinylidene fluoride (PVDF) are shown in Fig. 10a and Fig. 10b, respectively. A cusp-like behaviour in the frequency and temperature dependence of the real part of the permittivity $\varepsilon'(f, T)$ in the temperature range of T=-50–60°C accompanied by absorption maxima increasing and shifting towards higher temperatures with increasing frequency is related to a freezing of dipolar motion in the amorphous region. A dispersive ε' anomaly and absorption maxima shifting toward higher temperatures and increasing with increasing frequency in the range of T=60–100°C are ascribed to wide angle oscillations of dipoles attached to the chain, followed by their rotation with the main chain co-operation appearing in the crystalline phase.

The dielectric absorption behavior apparent in the range of T=-50–60°C is characteristic of the static dipolar freezing of dipolar motion in the absence of a long-range correlation. Dielectric absorption in the crystalline phase of the polymer observed in temperature range from T=60° to T=100°C is described by the oscillation motion of the VDF groups.

Temperature dependence of the real part permittivity ε' (a) and the imaginary part permittivity ε" (b) of BST60/40//PVDF composites with different concentrations of ceramics phase, for frequency f=100kHz is shown in Fig. 11. The permittivity ε' is higher in comparison with that of the polymer (Fig. 10) due to the high permittivity value of BST (Fig. 9). It should be observed that the temperature dependence of the dielectric

response of the polymer determines the response of the composites.

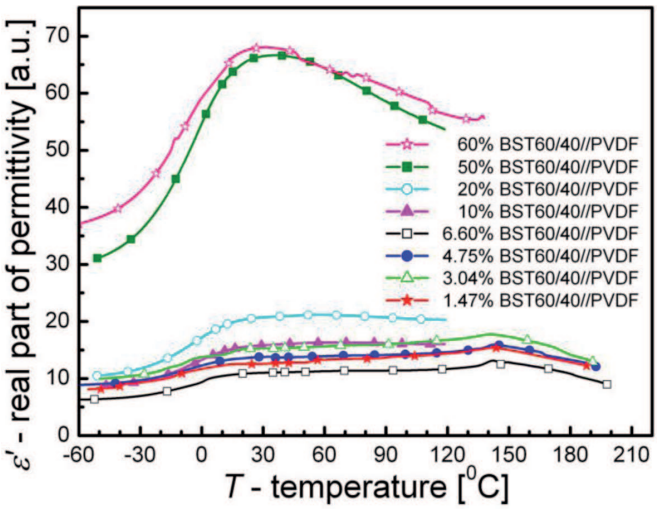

Fig. 11a. Temperature dependence of the real part of dielectric permittivity ε' for BST60/40//PVDF composites at f=100kHz

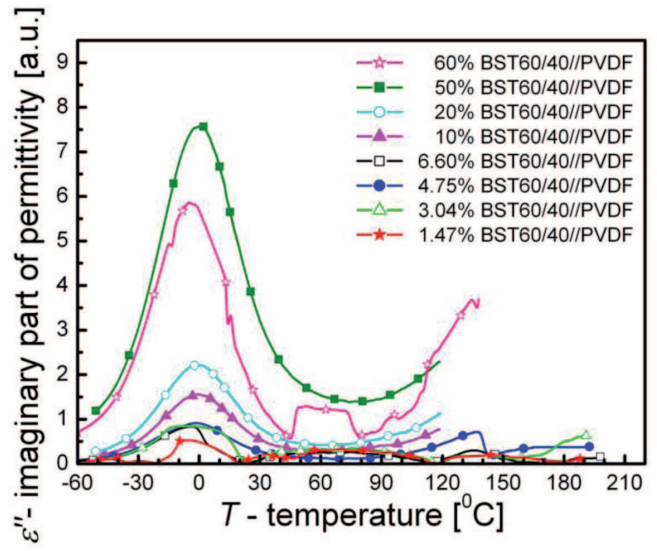

Fig. 11b. Temperature dependence of the imaginary part of dielectric permittivity ε" for BST60/40//PVC composites at f=100kHz

In the low temperature range the dielectric response of the composites is determined by the anomaly characteristic in the glass transition of the polymer, whereas in the high temperature range the relaxation related to the wide angle oscillation of the polymer polar groups followed by their rotation with main chain co-operation is dominant. The addition of the ceramics only slightly changes the dynamics of the α process in the polymer. The addition of the ceramics resulted in the increase thermal strength of the composites.

Frequency dependence of the maximum value of real part permittivity ε'_m for different content of the ceramic phase of BST60/40//PVDF is shown in Fig.12. With an increase in frequency the maximum value of the real part of permittivity ε'_m changes only slightly. One can see that the highest values of the real part of permittivity are observed for 50%BST60/40//PVDF and 60%BST60/40//PVDF composites. A small dependence on frequency has been found (Fig. 12).

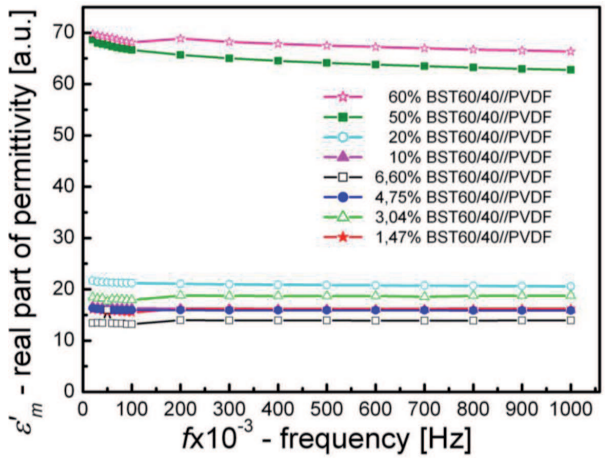

Fig. 12. Frequency dependence of the maximum value of ε'_m for different content of the ceramic phase for BST60/40//PVDF composites

Fig. 13 shows the dependence of the real part of permittivity ε'_m on the volume fraction of the ceramic phase for BST60/40//PVDF composite at f=50kHz, f=100kHz, f=500kHz and f=1MHz. One can see that the ε'_m of the composites increases with an increase in the volume fraction in the ceramic active phase. A small local maximum is seen in concentration at the active ceramic phase c_V=3.04%.

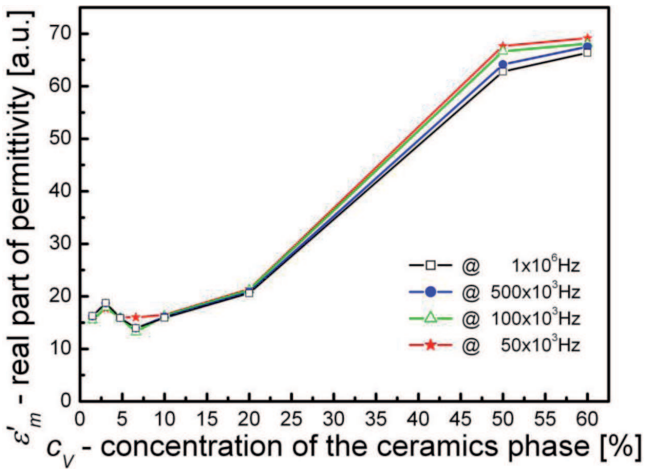

Fig.13. Dependence of the real part of dielectric permittivity ε'_m on the volume fraction of ceramic phase for BST60/40//PVDF composite at f=50kHz, f=100kHz, f=500kHz, f=1MHz

Dependence of the real ε' (a) and imaginary ε" (b) part of dielectric permittivity on volume fraction of the ceramic phase for BST60/40//PVDF in the mi-

crowave frequency range of f=3-10GHz at *RT* is given in Fig. 14.

One can see that a small amount of ceramic phases, i.e. $c_V \leqslant 10\%$ the real part of dielectric permittivity ε' is around 20. However, a peak of ε' can be see at c_V=4.75%, but with a further increase in the ceramic phase concentration, both ε' and ε'' increase.

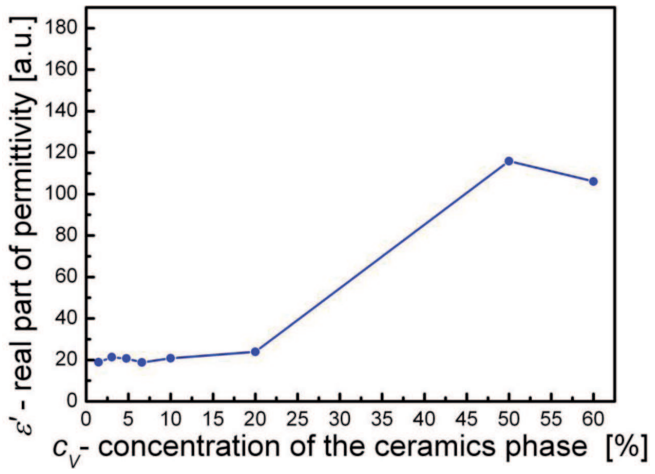

Fig. 14a. Dependence of the real part of dielectric permittivity ε' on the volume fraction of ceramic phase for BST60/40//PVDF composite in the microwave frequency range of f=3-10GHz at *RT*

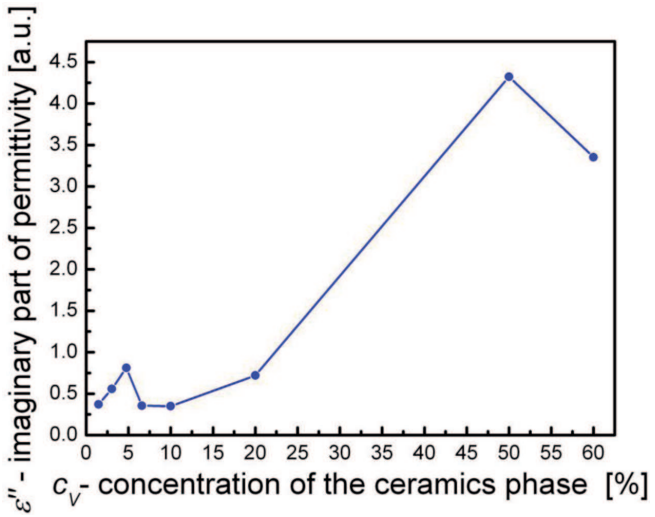

Fig. 14b. Dependence of the imaginary part of dielectric permittivity ε'' on the volume fraction of ceramic phase for BST60/40//PVDF composite in the microwave frequency range of f=3-10GHz at *RT*

It is was worth noting that the abrupt increase in dielectric permittivity has been observed in the ceramic-polymer composite with concentration of the active ceramic phase c_V >20% (Fig. 11a, Fig. 13, Fig. 14). It can be explained in the terms of percolation threshold. It is commonly known [9] that the percolation threshold may vary depending upon the matrix and dopant chemistries, particle sizes, shapes and spatial orientation as well as processing parameters. In case of high amounts of active ceramic phases in the ceramic-polymer composite it is possible that the percolation limit of the composite (in terms of the BST ceramic particles) may have been reached at this volume fraction. The direct conduction paths of ceramic material has been formed all the way both the top and bottom electrode of the pellet-like composite samples.

Taking into account results of the dielectric measurement performed for both low and high frequency of the measuring field one can conclude that the moderate permittivity observed (Fig. 11a) as well as low loss factor (Fig. 11b) of the composite. Satisfy the requirements for both piezoelectric applications as well as tunable microwave device design.

4. Conclusions

In the present study we have fabricated the electroactive ceramic-polymer composites of 0-3 connectivity using sol-gel derived barium strontium titanate $Ba_{0.6}Sr_{0.4}TiO_3$ fine powder and PVDF polymer powder by using a hot pressing method. Temperature and frequency dependence of the real and imaginary part of permittivity for ceramic-polymer composites with 0-3 connectivity show that dielectric properties are determined by the ceramic active phase (even at $c_V \sim 1\%$). It was found, that dielectric properties of the ceramic-polymer composite for c_V>20% change significantly in both small (f=10kHz-1MHz) and high (f=3-10GHz) frequencies. The abrupt increase in permittivity may indicate an excess percolation threshold, so the ceramic-polymer composite for concentration of the active ceramic phase c_V >20% cannot be indexed as composites with 0-3 connectivity. However, ceramic-polymer composites based on the BST active phase exhibited effectively diluted permittivity and low dielectric loss which improves microwave performance and possible piezoelectric applications.

Acknowledgements

The present research has been supported by Polish Ministry of Education and Science from the funds for science in 2011-2014 as a research project N N507 218540.

REFERENCES

[1] B. Hilczer, J. Kułek, E. Markiewicz, M. Kosec, B. Malic, Journal of Non- Crystalline Solids **305**, 167-173 (2002).

[2] K. Osińska, M. Adamczyk, D. Czekaj, Prace Komisji Nauk Ceramicznych-Polski Biuletyn Ceramiczny, Ceramika **101**, 125-131 (2008).
[3] B. Hilczer, J. Małecki, Elektrety i piezopolimery, PWN, Warszawa (1992).
[4] R.E. Newnham, D.P. Skinder, L.E. Cross, Materials Research Bulletin **13**(5), 325-336 (1978).
[5] K. Osińska, M. Adamczyk, D. Czekaj, Prace Komisji Nauk Ceramicznych- Polski Biuletyn Ceramiczny, Ceramika **103**, 245-252 (2008).
[6] K. Osińska, M. Adamczyk, M. Parcheniak, D. Czekaj, Archives of Metallurgy and Materials **54**, 985-997 (2009).
[7] B. Wodecka-Duś, A. Lisinska-Czekaj, T. Orkisz, M. Adamczyk, K. Osińska, L. Kozielski, D. Czekaj, Materials Science Poland **25**(3), 791-799 (2007).
[8] K. Osińska, J. Maszybrocka, J. Plewa, D. Czekaj, Archives of Metallurgy and Materials **54**, 911-922 (2009).
[9] B. Kumar, J.P. Fellner, Journal of Power Sources **123** 132-136 (2003).

Received: 20 April 2011.